CHRNA1 and its correlated-myogenesis/cell cycle genes are prognosis-related markers of metastatic melanoma

Mohamed Nabil Bakr [a,b], Haruko Takahashi [a,c,**], Yutaka Kikuchi [a,c,*]

[a] *Department of Biological Science, Graduate School of Science, Hiroshima University, Kagamiyama 1-3-1, Higashi-Hiroshima, Hiroshima, 739-8526, Japan*
[b] *National Institute of Oceanography and Fisheries (NIOF), Cairo, 11516, Egypt*
[c] *Graduate School of Integrated Sciences for Life, Hiroshima University, Kagamiyama 1-3-1, Higashi-Hiroshima, Hiroshima, 739-8526, Japan*

ARTICLE INFO

ABSTRACT

Nicotinic acetylcholine receptors (CHRNs) expression and their critical role in various types of cancer have been reported. However, it is still unclear which CHRNs and their associated genes play essential roles in metastasis in melanoma patients. Here, we performed bioinformatics analyses on publicly available bulk RNA sequencing (RNA-seq) data of patients with melanoma to identify the CHRNs highly expressed in metastatic melanoma. We found that CHRNA1 was highly expressed in metastatic melanoma samples compared to primary melanoma samples and was strongly associated with CHRNB1 and CHRNG. These muscle-type CHRNs (CHRNA1, CHRNB1, and CHRNG) were correlated with the ZEB1 and Rho/ROCK pathway-related genes in metastatic melanoma samples. Pairwise correlations and enrichment analyses revealed that CHRNA1 was significantly associated with myogenesis/muscle contraction and cell cycle genes. Kaplan-Meier curves illustrated the involvement of CHRNA1, four of its correlated genes (DES, FLNC, CDK1, and CDC20), and the myogenesis gene signature in the prognosis of melanoma patients. Following the bulk RNA-seq analysis, single-cell RNA-seq (scRNA-seq) analysis showed that the CHRNA1-expressing melanoma cells are primarily metastatic and had high expression levels of CHRNB1, CHRNG, and myogenesis/cell cycle-related genes. Our bioinformatics analyses of the bulk RNA-seq and scRNA-seq data of patients with melanoma revealed that CHRNA1 and its correlated myogenesis/cell-related cycle genes are critical prognosis-related markers of metastatic melanoma.

1. Introduction

Melanoma, caused by the malignant transformation of melanocytes, is a well-known severe type of skin cancer because it is highly invasive and metastatic [1,2]. Although melanoma is not an epithelial tumor, in the early stage of invasion, melanoma cells have been reported to undergo epithelial-mesenchymal transition (EMT)-like phenotype switching, which is orchestrated by EMT-inducing transcription factors (EMT-TFs), such as ZEB, TWIST, and SNAIL family proteins [3,4]. Melanoma phenotype switching by the transition to a dedifferentiated state has been thought to rarely cause various divergent differentiations, including rhabdomyosarcomatous differentiation, which expresses striated muscle genes at the metastatic sites [5]. After breaking the basement membrane, melanoma cells change their morphology and adopt three different migration modes (single cell, streaming, and collective modes) according to the surrounding environment [6,7]. The invasive front of melanoma is characterized by amoeboid movement, which is dependent on the contractility of actomyosin maintained by the Ras homolog gene family (RHO)/Rho-associated kinase (ROCK) and JAK/-STAT3 signaling pathways [6,7]. Many signaling pathways, such as TGF-β, Wnt, MAPK, and PI3K-AKT, have been reported to regulate tumor invasion and metastasis, including melanoma [1,8].

Acetylcholine (ACh), the first identified neurotransmitter, is known to regulate essential cell functions, such as cell differentiation, proliferation, and migration, as a signaling molecule in non-neuronal cells [9]. ACh signaling is transmitted through two types of ACh receptors: cholinergic receptor nicotinic α, β, γ, δ, and ε subunits (CHRNs), which are ligand-gated cation channels [10], and cholinergic receptor

muscarinic M (1–5) (CHRMs), which are G protein-coupled receptors [11]. Functional analysis of CHRMs in melanoma progression is limited to M3 [12], whereas the expression and detailed functional analysis of α5 and α9 CHRNs in melanoma cell lines have been reported [13]. CHRNs are classified into neuronal (α2 to α10 and β2 to β4) and muscular (α1, β1, γ, δ, and ε) receptors expressed in humans except for α8 [14,15]. Previously, CHRNs were thought to function only in the nervous system and at the neuromuscular junction; however, recent studies have reported that CHRNs and ACh are expressed in almost all types of cells, including cancer cells [9,10,15]. Since their first detection in lung cancer cells, CHRNs have been proven to be involved in tumor growth, metastasis, angiogenesis, and EMT [10,15]. Overexpression of *CHRNA9* induces breast cancer growth and metastasis through EMT [16]. *CHRNA7* stimulates lung cancer cell proliferation and invasion through the Ras/ERK/MAPK and JAK2/STAT/PI3K pathways [17], and the knockdown of *CHRNA5* inhibits the proliferation and invasion of the lung [18] and prostate cancers [19]. In melanoma cells, overexpression of *CHRNA5* promotes melanoma progression via Notch1, whereas knockdown of this receptor inhibits melanoma cell proliferation and invasion, as does inhibition of the PI3K/AKT and ERK1/2 signaling pathways [20]. *CHRNA9* stimulates melanoma cell proliferation and migration through the AKT and ERK signaling pathways [21]. While previous studies using cell culture systems have shown that specific CHRNs are crucial for the process of metastasis, a comprehensive bioinformatics analysis of which types of CHRNs play essential roles in metastatic melanoma has not yet been performed.

Rapid progress in sequencing technology has made it possible to analyze gene expression at the whole cancer cell or the single-cell level by using gene expression information from individual patients [22]. The Cancer Genome Atlas (TCGA), the world's largest publicly available database, provides genomic information, RNA sequencing (RNA-seq) data, and various clinical outcomes for over 30 human cancers (https://portal.gdc.cancer.gov/). In addition, recent studies using single-cell RNA sequencing (scRNA-seq) have demonstrated tumor heterogeneity, therapy resistance, and tumor and immune ecosystems in human patients [23–27]. Therefore, data-driven analyses that integrate bulk RNA-seq and scRNA-seq data are expected to discover new mechanisms in cancer. In this study, we performed combinational bioinformatics analyses for bulk RNA-seq and scRNA-seq data of patients with melanoma. We identified *CHRNA1* as the highest differentially expressed CHRNs in metastatic compared to primary melanoma patients obtained from the TCGA and GSE65904 datasets. In patients with metastatic melanoma, *CHRNA1* was significantly correlated to *ZEB1* EMT-TF, *RHO/ROCK* genes, and myogenesis/cell cycle-related genes. Survival analysis proved *CHRNA1* and its correlated genes as prognosis-related markers of metastatic melanoma. Additionally, single melanoma cells expressing *CHRNA1* were derived from metastatic sites and were enriched with myogenesis and cell cycle-related gene signatures.

2. Material and methods

2.1. Data collection

We used the R software (4.1.2) to perform all the bioinformatics analyses in this study. We retrieved the RNA-seq data and clinical characteristics of skin cutaneous melanoma (SKCM) patients from the TCGA database using the TCGABiolinks package (2.22.2) [28]. TCGA-SKCM samples included 103 primary melanoma and 367 metastatic melanoma samples. Another bulk RNA-seq dataset of patients with melanoma was obtained from the Gene Expression Omnibus (GEO) database (GSE65904) using the GEOquery package (2.62.2) [29]. There were 16 primary and 188 metastatic melanoma samples in the GSE65904 dataset. Furthermore, we used two melanoma scRNA-seq datasets (GSE115978 and GSE116237) to assign the characteristics of melanoma cells that expressed *CHRNA1*. Transcriptomic data of four

samples of rhabdomyosarcomatous melanoma were collected from a previous study [5].

2.2. Determination of the differentially expressed genes (DEGs)

TCGA-SKCM RNA-seq data in HTSeq-Counts format were used for the DEG analysis. DEGs between the metastatic and the primary TCGA-SKCM samples were identified using the edgeR package (3.36.0) [30]. The trimmed mean of M-values (TMM) method was used to normalize the HTSeq-count matrix. We considered log2FC > 1.5 and false discovery rate (FDR) < 0.05, to obtain significant DEGs. The ENSEMBL gene names were converted into gene symbols using the biomaRt package (v 2.50.2) [31].

2.3. Pairwise correlations

Pearson's r correlation test was performed to evaluate the correlations between the expression levels of the different CHRNs in TCGA-SKCM and GSE65904 datasets. Correlation matrices were visualized using the psych package (2.1.9) (https://cran.r-project.org/web/packages/psych/index.html). Additionally, pairwise correlations between muscle-type CHRNs expressions and *ZEB1* EMT-TF and Rho/ROCK pathway-related genes (*RHOA*, *RHOB*, *RHOC*, *ROCK1*, and *ROCK2*) expressions in metastatic melanoma samples were analyzed. We considered p-value <0.05 and ($r \leq -0.1$ |$r \geq 0.1$) for significant correlations. We identified the genes correlated with *CHRNA1* in TCGA-SKCM patients under p-value <0.05 and $r \geq 0.3$.

2.4. Enrichment analysis

Genes significantly correlated with *CHRNA1* (p-value <0.05 and $r \geq 0.3$) were used for enrichment analysis. Gene Ontology (GO) enrichment analysis (Biological process) was performed using the enrichR (3.0) interface of the Enrichr database [32]. To perform gene set enrichment analysis (GSEA) of cancer hallmarks, we used the fgsea package (1.20.0) [33]. A line enrichment plot for the HALLMARK_MYOGENESIS pathway was visualized using the plotEnrichment function.

For protein-protein interaction (PPI) analysis, *CHRNA1*-correlated genes were analyzed using Cytoscape software (v 3.9.1) [34]. We used the built-in StringApp [35] to construct a PPI network and reclaim the functional enrichment of the *CHRNA1*-correlated genes. The densely interconnected regions within our PPI network were clustered using the molecular complex detection (MCODE) algorithm [36], and four PPI subnetworks (node >3) were identified.

2.5. Survival analysis

We employed the R2: Genomics Analysis and Visualization Platform (http://r2.amc.nl) to investigate the correlation of *CHRNA1* to the survival of patients with metastatic melanoma using the GSE19234 dataset and scan cutoff mode. Genes included in the MCODE PPI subnetworks were explored for their relationships with survival in melanoma patients. Overall survival analyses based on the median expression cutoff were performed using the Gene Expression Profiling Interactive Analysis (GEPIA) tool [37]. Kaplan-Meier survival curves were constructed for the chosen genes, and hazard ratios (HRs) based on the Cox proportional-hazards (PH) model and log-rank p-values were calculated. A p-value <0.05 was considered significant. TCGA-SKCM samples were classified into five groups based on the stage of the melanoma (Stages 0, I, II, III, and IV). To create a survival object, we used the Surv function from the Survival package (3.2–13) (https://cran.r-project.org/web/packages/survival/index.html). Then, the survival curve was fitted separately by melanoma stages using the survfit function. The log-rank test was used to examine the survival distribution of the melanoma stage groups, and a p-value <0.05 was considered significant. Finally, the Kaplan-Meier curve was visualized using the ggsurvplot function from

the Survminer package (0.4.9) (https://cran.r-project.org/web/packages/survminer/index.html).

2.6. The scRNA-seq analysis

The GSE115978 scRNA-seq dataset contained 2018 malignant cells out of 7186 cells from 31 patients with melanoma [27]. Only the count matrices of melanoma cells expressing *CHRNA1* were isolated and analyzed using the Seurat package (4.0.4) [38]. We filtered cells with fewer than 200 genes and mitochondrial counts >5%. Cells of different patients were integrated using canonical correlation analysis, normalized using the LogNormalize method, and scaled. Principal component analysis (PCA) was performed using ten ncps and cells clustered with 0.4 resolution. Two clusters were recognized and represented using UMAP (dims = 1:10). We used the Wilcoxon rank-sum test to identify marker genes of the two recognized scRNA clusters. To perform the GSEA of cancer hallmarks, we used the GSVA package (1.42.0) [39], and the pheatmap package (1.0.12) (https://cran.r-project.org/web/packages/pheatmap/index.html) was used to visualize the results. The cell cycle phases of each cluster's cells were addressed based on G2/M and S markers expressions using the CellCycleScoring function [25]. For validation, an extra scRNA-seq dataset (GSE116237) was analyzed. The GSE116237 dataset comprised 674 cells from patient-derived xenograft (PDX) models [26]. We followed the default protocol of the Seurat package, and cells with fewer than 200 genes and mitochondrial counts >5% were excluded. We identified six clusters of melanoma cells at 0.3 resolution. The cell clusters were visualized using UMAP (dims = 1:10).

2.7. Profiling of the muscle-related genes in rhabdomyosarcomatous melanoma and TCGA-SKCM samples

We merged the HTSeq-FPKM expressions of the TCGA-SKCM samples and the transcripts per kilobase million (TPM) expressions of the rhabdomyosarcomatous melanoma samples into one matrix after trimming the unshared genes. High and low *CHRNA1*-expressing TCGA samples were identified based on the median expression cutoff value of the *CHRNA1*. The log2 values were calculated to unify the scale of the merged expression matrix. Then the expressions of the muscle-related genes were compared and visualized using the ComplexHeatmap package (2.10.0) [40].

3. Results

3.1. CHRNA1 showed higher expression levels in metastatic than primary melanomas

To investigate the expression of CHRNs and their roles in melanoma metastasis, we performed comprehensive computational analyses on human melanoma samples obtained from publicly available databases. Differential gene expression analysis between 367 metastatic and 103 primary melanoma samples obtained from the TCGA-SKCM database identified 1382 DEGs with log2FC > 1.5 and FDR <0.05. We detected 12 of the 16 CHRNs among the DEGs (Table 1). Interestingly, *CHRNA1* showed the highest difference in expression between metastatic and primary melanomas with log2FC > 1.5 (p-value = 1.07×10^{-5}) (Table 1 and Fig. 1A). We further found in another independent dataset (GSE65904) that *CHRNA1* expression in metastatic melanoma was significantly higher than that in primary melanoma (p-value = 0.0065) (Fig. 1B). In addition, melanoma patients with high *CHRNA1* expression were significantly correlated with late melanoma stages (stages III and IV) (p-value = 0.024) (Fig. 1C) and with a high rate of spread to lymph nodes (N3) (p-value = 0.038) (Fig. 1D). Altogether, our results reveal that muscle-type *CHRNA1* is associated with metastasis of human melanoma.

Table 1

Differentially expressed CHRNs in metastatic vs. primary TCGA-SKCM samples.

CHRNs	log2FC	logCPM	*p*-value
CHRNA1	1.557	3.299 E+00	1.070E-05
CHRNA3	0.867	−2.122E-01	3.380E-04
CHRNA5	0.133	1.719 E+00	2.771E-01
CHRNA6	1.033	1.865 E+00	1.495E-03
CHRNA7	0.126	−1.026 E+00	6.064E-01
CHRNA9	0.422	−3.998E-02	2.948E-01
CHRNA10	−0.653	−5.548E-01	3.360E-08
CHRNB1	−0.229	3.180 E+00	9.781E-03
CHRNB2	−0.615	2.237 E+00	1.982E-02
CHRNB4	0.271	−5.207E-01	3.054E-01
CHRND	1.189	−1.708 E+00	5.634E-04
CHRNE	−0.187	1.199 E+00	3.396E-01

3.2. Correlations of muscle-type CHRNs with EMT-TFs- and Rho/ROCK pathway-related genes in melanoma patients

To determine which CHRNs are associated with *CHRNA1* in melanoma patients, Pearson's correlation test was applied to TCGA-SKCM and GSE65904 samples (Fig. 2). We found that both *CHRNB1* and *CHRNG* were significantly correlated with *CHRNA1* (p-value <0.001) in metastatic melanoma samples (Fig. 2A and B). To further investigate the involvement of these muscle-type CHRNs (*CHRNA1*, *CHRNB1*, and *CHRNG*) in human melanoma metastasis, we analyzed the pairwise correlations between these CHRNs and EMT-TFs expressions in patients with metastatic melanoma. We found that the expressions of the three CHRNs were positively correlated with *ZEB1* expression in both TCGA-SKCM and GSE65904 samples (Fig. 2C). Besides, we examined the correlation between the three CHRNs and the Rho GTPase (*RHOA*, *RHOB*, and *RHOC*)/ROCK (*ROCK1* and *ROCK2*) genes in metastatic melanoma samples to determine their involvement in melanoma movement. Results showed that some *RHO/ROCK* genes were correlated with individual CHRNs (*CHRNA1*, *CHRNB1*, and *CHRNG* were correlated with *RHOA/RHOC*, *RHOB/ROCK1/ROCK2*, and *ROCK2*, respectively) (Fig. 2D). These findings explain the crucial role of *CHRNA1*, *CHRNB1*, and *CHRNG* in melanoma movement metastasis.

3.3. GO, GSEA, and PPI analyses of CHRNA1-correlated genes in melanoma

Genes positively correlated with *CHRNA1* were identified under r ≥ 0.3 and *p*-value <0.05. The identified *CHRNA1*-correlated genes were presented for enrichment analyses to investigate their biological functions (Fig. 3). GO enrichment (Biological process) analysis showed that genes correlated with *CHRNA1* were mainly associated with muscle and heart contraction (*p*-value <0.05) (Fig. 3A). Furthermore, the GSEA of cancer hallmarks confirmed the association with myogenesis (*p*-value <0.05) (Fig. 3B). Next, we performed PPI analysis for *CHRNA1*-correlated genes to explore their functional interactions. Further, we applied the MCODE algorithm to determine the highly connected PPIs (Fig. 3C). Consistent with GO enrichment and GSEA results, the top four MCODE PPI networks were muscle contraction/development, muscle development, cytoskeleton/sarcolemma, and cell cycle-related networks (Fig. 3C). These results revealed that the expression of *CHRNA1* in melanoma patients is correlated with genes related to myogenesis, muscle contraction, and cell cycle.

3.4. CHRNA1, its correlated genes, and myogenesis signature were correlated to melanoma prognosis

Kaplan-Meier analysis for patients with metastatic melanoma using the R2 online platform revealed that patients with high expression of *CHRNA1* had a poorer prognosis than patients with low *CHRNA1* expression (*p*-value = 0.036) (Fig. 4A). Additionally, Among the *CHRNA1*-correlated genes in the MCODE PPI networks, we found that
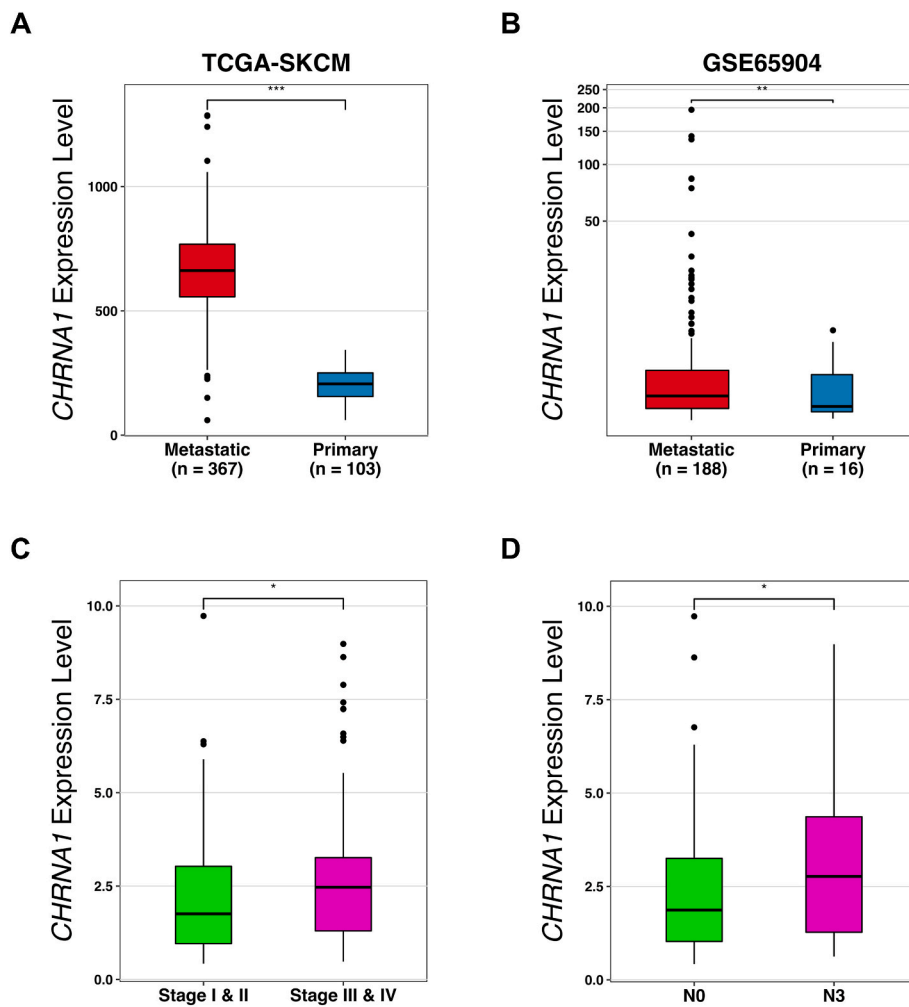
A

B

C

D

Fig. 1. *CHRNA1* expression level is higher in metastatic versus primary melanomas. (A, B) Box plots for the *CHRNA1* differential expression between metastatic and primary melanomas from TCGA-SKCM (A) and GSE65904 datasets (B). (C, D) Box plots for TCGA-SKCM patients with high *CHRNA1* expression levels (expression > median value) grouped by pathological stages (C) and N classification (D). * p-value <0.05, ** p-value <0.01, and *** p-value <0.001 according to Student t-Tests. N = tumor spread degree to lymph nodes.

DES, *CDK1*, *CDC20*, and *FLNC* were prognosis-related genes (log-rank p-value <0.05) (Fig. 4B). Since patients with high *CHRNA1* expression were associated with late-stage melanoma (Fig. 1C), we investigated the correlation between melanoma stage and patient survival. Patients with melanoma stages III and IV had a poorer prognosis than patients with melanoma at the early stages (0, I, and II) (log-rank p-value = 0.0008) (Fig. 4C). By comparing the gene signature of every melanoma stage, we found that late-stage (III and IV) melanomas were enriched with myogenesis, angiogenesis, and EMT characteristics (Fig. 4D).

3.5. Analysis of CHRNA1-expressing melanoma cells using scRNA-seq

Using bulk RNA-seq data, *CHRNA1* expression was shown to be correlated with the expressions of myogenesis- and cell cycle-related genes. We next investigated the characteristics of melanoma cells expressing *CHRNA1* at the single-cell level. We re-analyzed the publicly available scRNA-seq dataset (GSE115978) of patients with melanoma (Fig. 5 and Fig. S1). First, we isolated 138 melanoma cells that expressed *CHRNA1*. The *CHRNA1*-expressing melanoma cells were represented in two clusters (clusters 0 and 1) (Fig. 5A). These cells were derived from 12 melanoma patients (Fig. S1A) and were mainly metastatic cells (Fig. S1B). The expressions of the top 10 marker genes of each scRNA cluster confirmed that these two clusters (clusters 0 and 1) had different gene expression profiles (Fig. S1C). The muscle-type CHRNs (*CHRNA1*, *CHRNB1*, and *CHRNG*) showed higher expressions in cluster 1 than in cluster 0 (Fig. 5B). Additionally, GSEA of cancer hallmarks revealed that cluster 1 cells were highly enriched with myogenesis, G2M checkpoint,

and mitotic spindle (Fig. 5C). In line with these results, 56% of cluster 1 cells were in the G2M cell cycle phase (Fig. 5D). These results suggest that *CHRNA1* expression correlates with the expression of myogenesis- and cell cycle-related genes. Similar results were obtained by analyzing another scRNA-seq dataset (GSE116237) (Fig. S2). One cluster of melanoma cells (cluster 5) showed the highest expression level of *CHRNA1* (Fig. S2B), and this cluster was enriched with myogenesis, EMT, and angiogenesis signatures (Fig. S2C).

3.6. Comparison of muscle-related gene expression between CHRNA1-expressing melanoma and rhabdomyosarcomatous melanoma

Previous studies have revealed that melanoma can change into various differentiation states, owing to its high cellular plasticity. One of these differentiated states has been reported to be rhabdomyosarcomatous melanoma, which has been shown to express many muscle-related genes. To determine whether melanomas with high expression of *CHRNA1* have similar gene expression profiles to rhabdomyosarcomatous melanoma, we compared the expressions of the identified muscle-related genes that correlate with *CHRNA1* in both TCGA-SKCM samples and rhabdomyosarcomatous melanoma samples (Fig. 6). 27 and 12 muscle-related genes were identified from TCGA-SKCM and scRNA-seq data as *CHRNA1*-correlated genes, respectively, of which only five genes were overlapped (Fig. 6A). We compared the expression of the 34 muscle-related genes between rhabdomyosarcomatous melanoma and high and low *CHRNA1*-expressing TCGA-SKCM samples (Fig. 6B). We found that the expression levels of almost all the muscle *CHRNA1*-
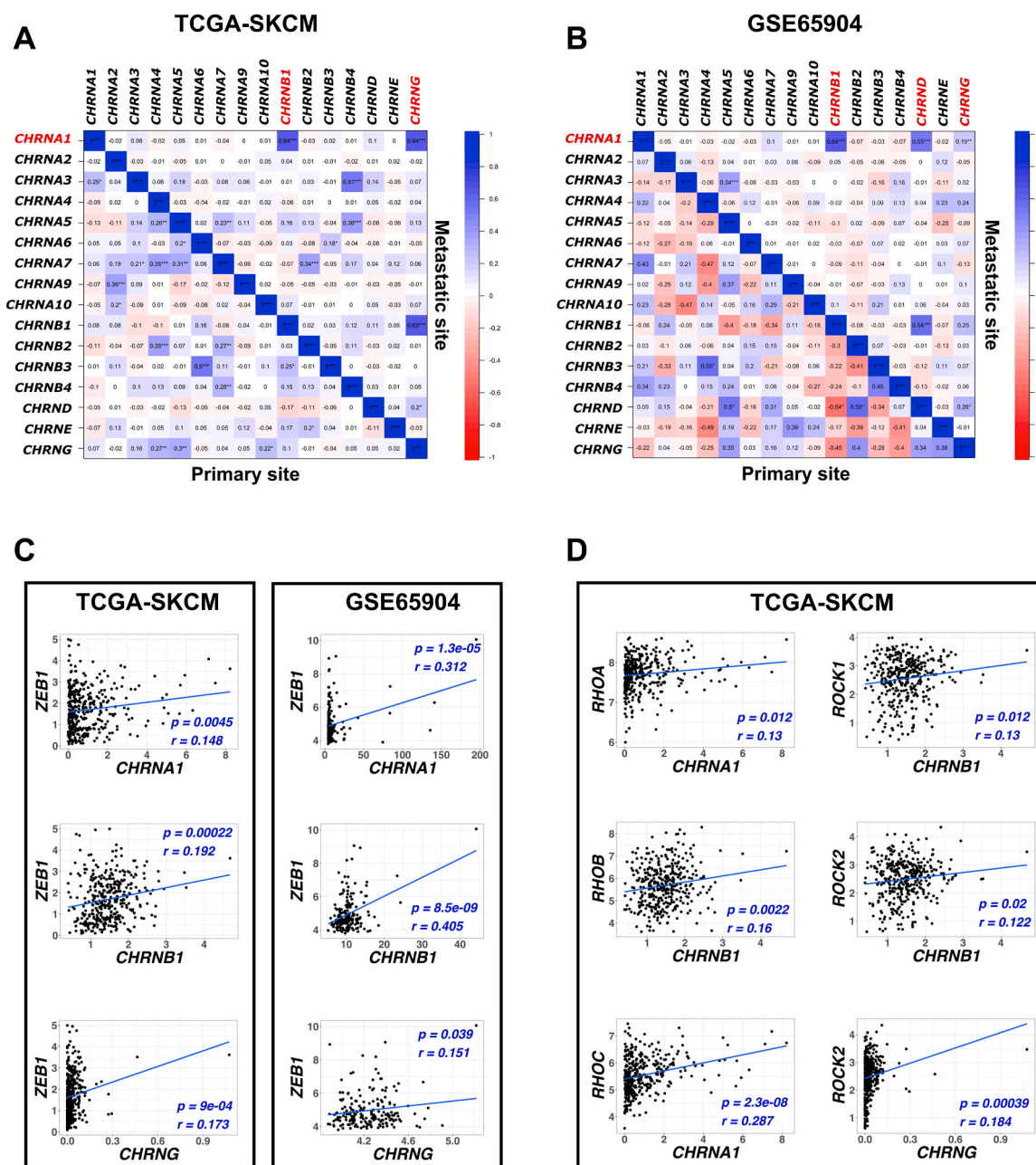
Fig. 2. *CHRNA1* highly correlates to *CHRNB1* and *CHRNG*, and these muscle-type CHRNs correlate with *ZEB1* EMT-TF and Rho/ROCK pathway-related genes in metastatic melanoma patients. (A, B) Correlation matrices (Pearson's correlation test r ≤ −0.1 |r ≥ 0.1) for CHRNs mRNA expressions in metastatic and primary TCGA-SKCM samples (A) and GSE65904 samples (B). * *p*-value <0.05, ** *p*-value <0.01, and *** *p*-value <0.001 according to Student t-Tests. (C, D) Pairwise scatter plots for the correlation between the expressions of muscle-type CHRNs and *ZEB1* (C) and *RHO/ROCK* genes expressions (D). Significant correlation based on *p*-value <0.05 and Pearson's correlation test (r ≤ −0.1 |r ≥ 0.1). A blue-colored line representing the linear regression for best curve fitting was drawn. (For interpretation of the references to color in this figure legend, the reader is referred to the Web version of this article.)

correlated genes were lower in melanoma than that in rhabdomyo-sarcomatous melanoma samples (Fig. 6B). Moreover, some muscle *CHRNA1*-correlated genes (*DES*, *SLN*, *TNNI2*, and *TNNC1*) showed higher expression in the high *CHRNA1*-expressing TCGA-SKCM samples than in the samples with low expression of *CHRNA1* (Fig. 6B). These results indicate that *CHRNA1*, together with the following genes (*DES*, *SLN*, *TNNI2*, and *TNNC1*), may function in the melanoma differentiation process to the rhabdomyosarcomatous melanoma state.

4. Discussion

Nicotine, the primary component in tobacco, causes health problems

and is well known for its malignant effects on various cancers [10]. Nicotine has been reported to act on cancer cells mainly through CHRNs. Previous studies using cancer cell lines have shown that nicotine treatment promotes the malignant transformation of tumors while blocking the expression of CHRNs or antagonist treatment results in the inhibition of tumor progression [10,17–21]. Recently, *CHRNA5* [20] and *CHRNA9* [21] were implicated in melanoma progression and migration in melanoma cell lines. In this study, to analyze the type and role of CHRNs in melanoma metastasis, we used *in silico* analysis of human melanoma samples obtained from TCGA-SKCM and GSE65904 datasets. By analyzing these samples, we found that among the 16 CHRNs expressed in humans, *CHRNA1*, but not *CHRNA5* and *CHRNA9*, showed the
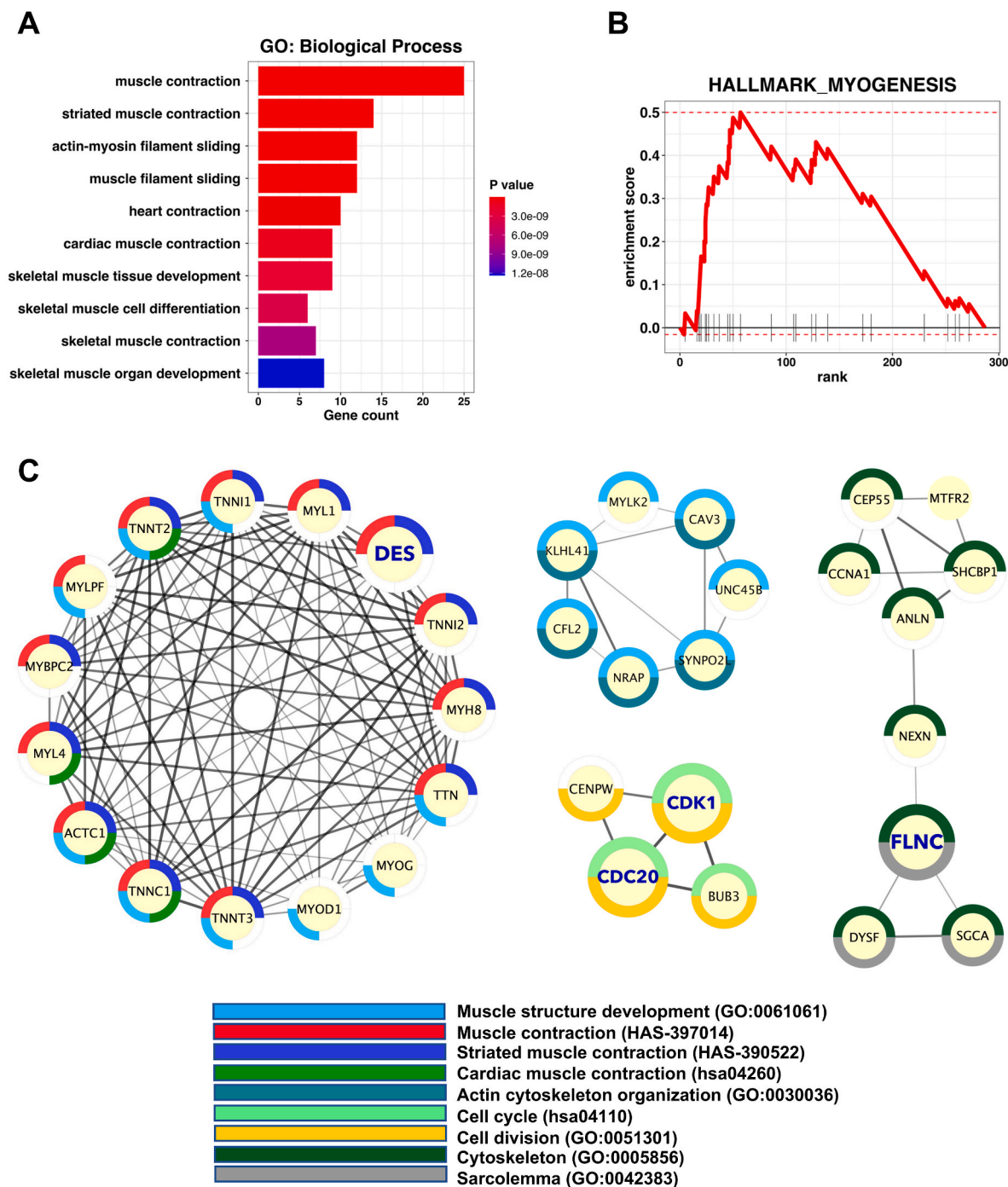
Fig. 3. Enrichment analysis for genes significantly correlated to CHRNA1 in metastatic TCGA-SKCM patients. (A) Bar plot showing GO enrichment (Biological Process) analyses for CHRNA1-correlated genes ($r \geq 0.3$ and *p*-value <0.05). (B) Line enrichment plot for the GSEA of HALLMARK_MYOGENESIS. (C) MCODE densely connected PPI clusters with enrichment retrieved by StringApp.

highest differential expression in metastatic melanoma samples. Although overexpression of *CHRNA1* has been reported in early-stage lung adenocarcinoma [41,42], head and neck squamous cell carcinoma (SCC) [43], and glioblastoma multiforme (GBM) tumors [44], our study is the first to confirm its high expression in metastatic melanoma.

Phenotype switching, an EMT-like process, has been described in melanoma, driven by EMT-TFs [3,4]. In the current study, *CHRNA1* was significantly correlated with *CHRNB1* and *CHRNG* in metastatic melanoma samples. Furthermore, we found that the expressions of *CHRNA1*, *CHRNB1*, and *CHRNG* were significantly correlated with the expression of *ZEB1* EMT-TF. *ZEB1* has been reported to be a critical regulator for

melanoma phenotype switching [3,45]. *ZEB1* showed increased expression during melanoma progression, and its overexpression was correlated with poor prognosis and therapy resistance in melanoma patients [45–48]. On the other hand, the knockdown of *ZEB1* decreased the invasiveness and inhibited the growth of melanoma cells [45,46]. Another interesting observation in our research was the significant correlation between the expressions of these muscle-type CHRNs and Rho/ROCK pathway-related genes, which play a crucial role in tumor migration [6]. Previous studies have revealed that *CHRNA9* and mouse *chrna7* regulate *TWIST1* in breast cancer cell lines and RhoA activation in neural cell lines, respectively [16,49]. Our results suggest that
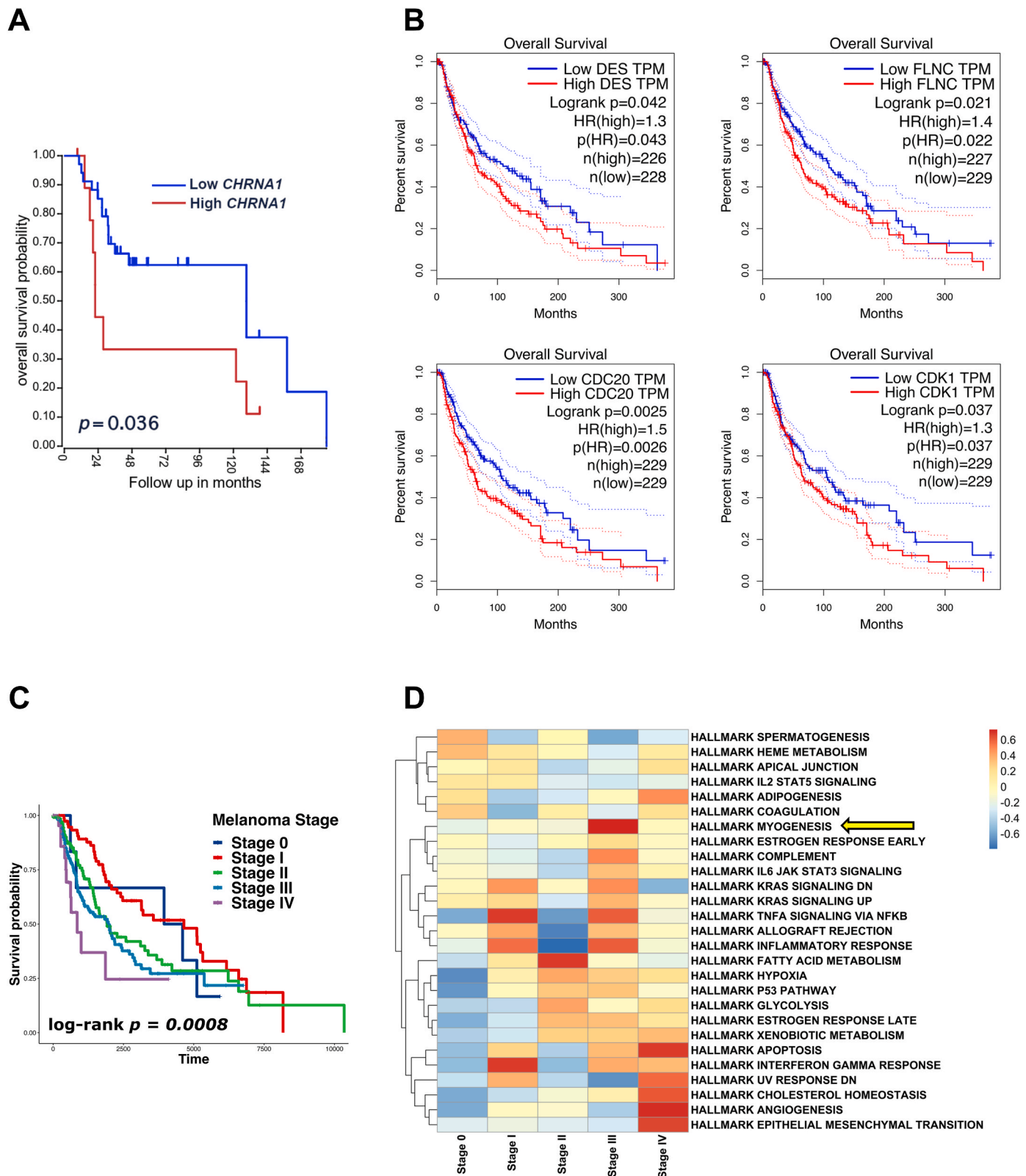
Fig. 4. CHRNA1 and its correlated genes are linked to prognosis in melanoma. (A) Kaplan-Meier survival curve for *CHRNA1* in metastatic melanoma patients based on the R2 platform (http://r2.amc.nl) analysis. (B) Kaplan-Meier survival curves for genes derived from the highly interconnected (CHRNA1-correlated genes) MCODE PPIs. (C) Kaplan-Meier survival curve for TCGA-SKCM patients within different melanoma stage groups. (D) Heatmap showing the GSEA of cancer hallmarks among the different melanoma stage groups. Yellow arrow pointing to the hallmark myogenesis enrichment. (For interpretation of the references to color in this figure legend, the reader is referred to the Web version of this article.)
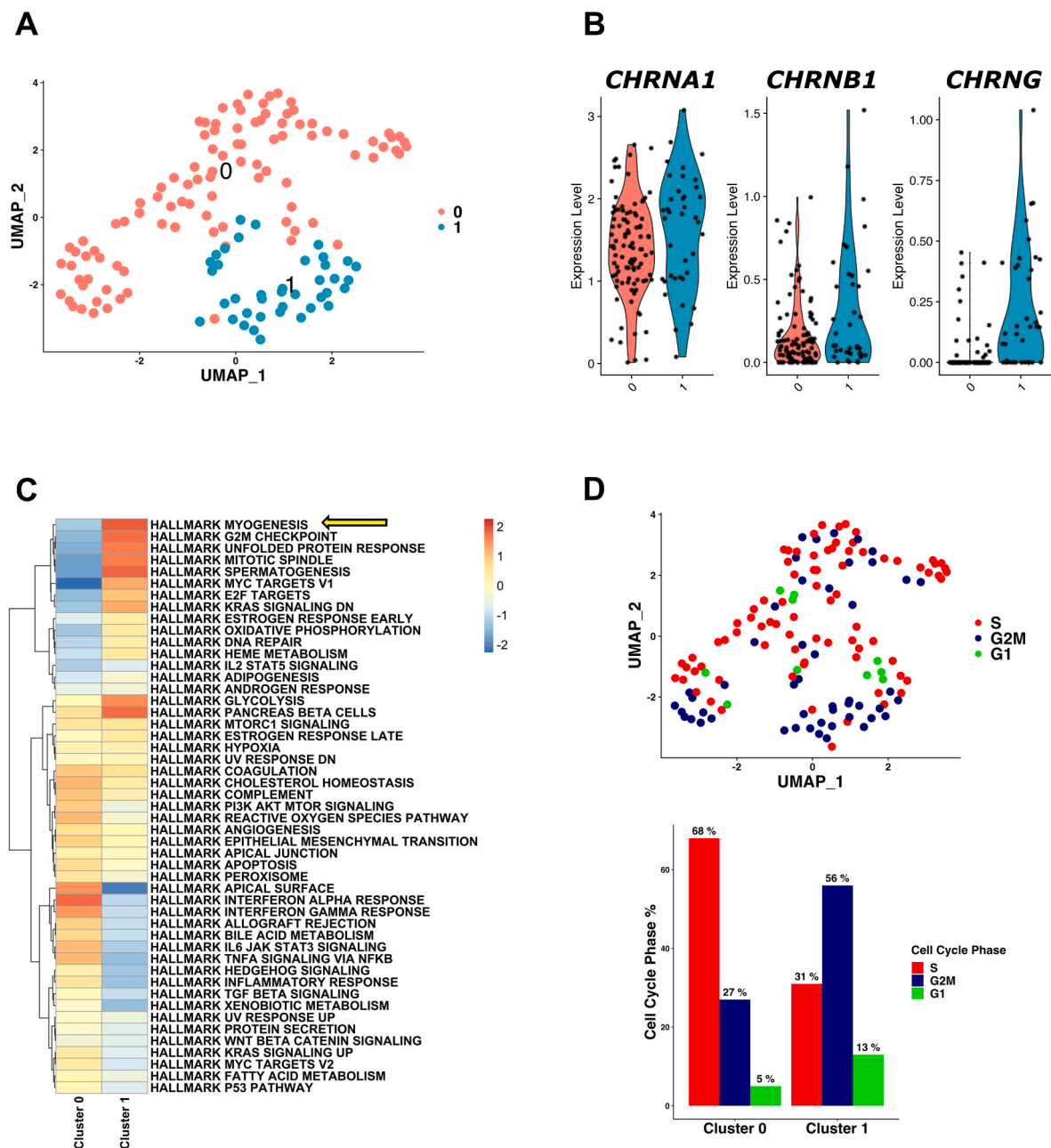
Fig. 5. Melanoma cells expressing CHRNA1 at the scRNA-seq level had a myogenesis gene signature. (A) UMAP plot representing clusters (0 and 1) of single cells from the GSE115978 scRNA-seq dataset. (B) Violin plots for *CHRNA1*, *CHRNB1*, and *CHRNG* expressions in the scRNA clusters. (C) Heatmap demonstrates the characteristic GSEA of cancer hallmarks for each scRNA cluster. Yellow arrow pointing to the hallmark myogenesis enrichment. (D) UMAP plot (upper) of the cell cycle phases (S, G2M, and G1) and their percentages (lower bar plot) across the scRNA clusters. (For interpretation of the references to color in this figure legend, the reader is referred to the Web version of this article.)

muscle-type CHRNs may be directly involved in melanoma metastasis via regulation of *ZEB1* EMT-TF expression and Rho/ROCK pathway activation.

Enrichment and pathway analyses of genes correlated with *CHRNA1* showed that these genes are involved in myogenesis, muscle contraction, and cell proliferation. *CHRNA1* and four correlated genes (*DES*, *CDK1*, *CDC20*, and *FLNC*) were associated with poor prognosis in metastatic melanoma patients. Recurrence-free and overall survival analyses revealed that high expression of *CHRNA1* was correlated with reduced survival in patients with lung adenocarcinoma [41] and glioblastoma [44]. *DES* gene encodes Desmin, an intermediate filament muscle-specific protein functioning in several types of cancer [5,50–53]. High *Desmin* expression has been reported in rhabdomyosarcomatous

melanoma [5] and colorectal tumors [51,53]. In contrast, patients with gallbladder cancer have lower expression levels of *Desmin* in cancerous tissues compared to non-tumor tissues owing to epigenetic dysregulation [52]. Consistent with our findings, overexpression of *Desmin* was associated with poor prognosis [51] and advanced stages [53] in patients with colorectal cancer. Upregulation of *CDK1* [54] and *CDC20* [55] genes has been reported in various cancers and linked to poor prognosis [56]. *FLNC* gene encodes Filamin-C, an actin-binding protein involved in the metastasis cancer cells [57]. Overexpression of *FLNC* was associated with progression, metastasis, and poor prognosis in hepatocellular carcinoma [58], esophageal squamous cell carcinoma [59], and glioblastoma [57]. Consistent with the bulk RNA-seq outputs, using scRNA-seq analysis, we found that myogenesis and cell proliferation
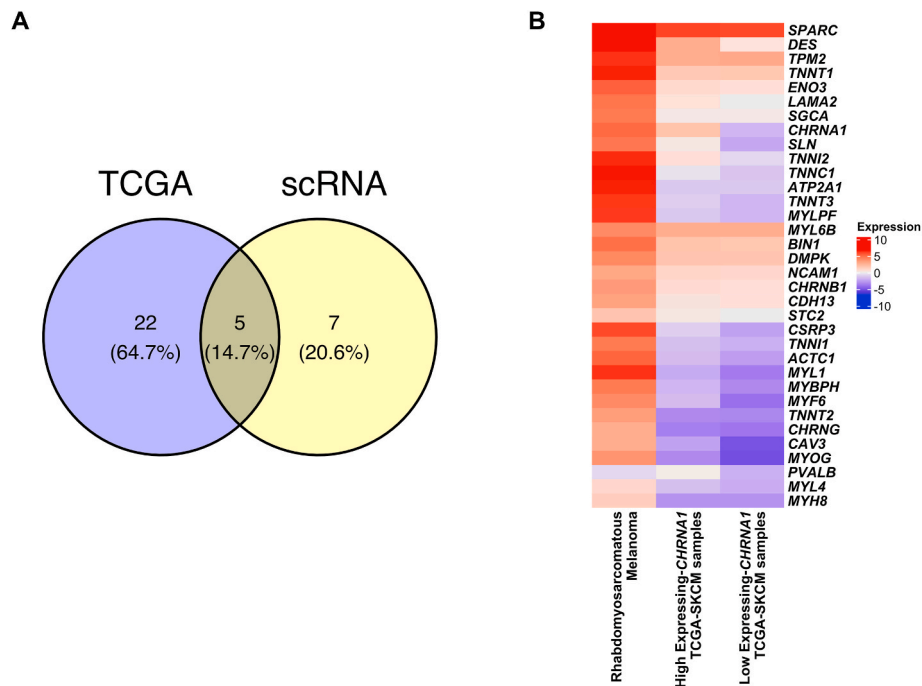
Fig. 6. Melanoma samples with high CHRNA1 expression have a profile quite similar to patients with rhabdomyosarcomatous melanoma. (A) Venn diagram represents the muscle-related genes enriched in samples with *CHRNA1* high expression from TCGA-SKCM and the GSE115978 scRNA-seq datasets. (B) Heatmap showing the expression of the muscle-related genes in high & low *CHRNA1*-expressing TCGA-SKCM samples and the rhabdomyosarcomatous melanoma samples.

gene signatures were enriched in cells expressing *CHRNA1*.

Accumulating evidence from recent experiments has shown increased expression of sarcomeric proteins, such as Myosin, Titin, MyBP-C, Obscurin, ACTN, Nebulin, Synemin, Desmin, Plectin, Nesprin, and Vimentin, in various cancers, and their overexpression has been reported to be associated with the malignant transformation of cancer [50]. In normal cells of the body, these proteins function in skeletal and cardiac muscles to contract using sarcomere structures, whereas, in cancer cells, they are thought to be involved in invasion and migration for metastasis. In our study, the *CHRNA1*-correlated myogenesis/sarcomere genes, including *MYOG*, *MYH8*, and *DES*, were highly expressed in metastatic melanoma, similar to rhabdomyosarcomatous melanoma. These results suggested that their expression may be involved in melanoma malignancy. In the future, the significance of *CHRNA1* and sarcomeric gene expression in the malignant transformation of melanoma should be further investigated. Our analysis demonstrated the involvement of the *CHRNA1* and its correlated myogenesis/cell cycle-related genes in melanoma metastasis and prognosis. However, further experimental confirmation of the role of *CHRNA1* expression in melanoma progression should be carried out. For instance, *CHRNA1* knockout or knockdown experiments *in vivo* or *in vitro* could be conducted. Immunostaining of clinical tissue samples and real-time PCR (RT-qPCR) studies would be advantageous to confirm both the *CHRNA1* expression as well as the association between *CHRNA1* and identified correlated genes in patients with melanoma.

5. Conclusion

In conclusion, our bioinformatics analysis of melanoma patients revealed that *CHRNA1* was highly expressed in metastatic melanoma and was correlated with *CHRNB1* and *CHRNG*. Moreover, the expression of muscle-type CHRNs (*CHRNA1*, *CHRNB1*, and *CHRNG*) was significantly correlated with *ZEB1* EMT-TF and Rho/ROCK pathway-related genes. The gene profile of *CHRNA1*-expressing metastatic melanoma patients and single melanoma cells showed a high enrichment of myogenesis/cell cycle-related genes. *CHRNA1*, its correlated genes, and

myogenesis signature correlated with prognosis in melanoma patients. Our results reveal that *CHRNA1* may function in melanoma metastasis and, together with its correlated myogenesis/cell cycle genes, are critical prognosis-related markers of metastatic melanoma.

Declaration competing of interest

The authors declare the following financial interests/personal relationships which may be considered as potential competing interests: Mohamed Nabil Bakr reports financial support was provided by Ministry of Higher Education, Egypt.

Appendix A. Supplementary data

Supplementary data to this article can be found online at https://doi.org/10.1016/j.bbrep.2023.101425.

References

[1] D. Schadendorf, D.E. Fisher, C. Garbe, J.E. Gershenwald, J.-J. Grob, A. Halpern, M. Herlyn, M.A. Marchetti, G. McArthur, A. Ribas, A. Roesch, A. Hauschild, Melanoma., Nat Rev Dis Primers. 1 (2015), 15003, https://doi.org/10.1038/nrdp.2015.3.

[2] A.J. Miller, M.C. Mihm, Melanoma, N. Engl. J. Med. 355 (2006) 51–65, https://doi.org/10.1056/NEJMra052166.

[3] Y. Tang, S. Durand, S. Dalle, J. Caramel, EMT-inducing transcription factors, drivers of melanoma phenotype switching, and resistance to treatment, Cancers (Basel) 12 (2020), https://doi.org/10.3390/cancers12082154.

[4] D. Pedri, P. Karras, E. Landeloos, J.C. Marine, F. Rambow, Epithelial-to-mesenchymal-like transition events in melanoma, FEBS J. 289 (2022), https://doi.org/10.1111/febs.16021.

[5] I. Ferreira, A. Droop, O. Edwards, K. Wong, V. Harle, O. Habeeb, D. Gharpuray-Pandit, J. Houghton, K. Wiedemeyer, T. Mentzel, S.D. Billings, J.S. Ko, L. Füzesi, K. Mulholland, I.K. Prusac, B. Liegl-Atzwanger, N. de Saint Aubain, H. Caldwell, L. Riva, L. van der Weyden, M.J. Arends, T. Brenn, D.J. Adams, The clinicopathologic spectrum and genomic landscape of de-/trans-differentiated melanoma, Mod. Pathol. 34 (2021), https://doi.org/10.1038/s41379-021-00857-z.

[6] P. Pandya, J.L. Orgaz, V. Sanz-Moreno, Modes of invasion during tumour dissemination, Mol Oncol 11 (2017), https://doi.org/10.1002/1878-0261.12019.

[7] A.G. Clark, D.M. Vignjevic, Modes of cancer cell invasion and the role of the microenvironment, Curr. Opin. Cell Biol. 36 (2015), https://doi.org/10.1016/j.ceb.2015.06.004.

[8] H. He, X. Shao, Y. Li, R. Gihu, H. Xie, J. Zhou, H. Yan, Targeting signaling pathway networks in several malignant tumors: progresses and challenges, Front. Pharmacol. 12 (2021), https://doi.org/10.3389/fphar.2021.675675.

[9] I. Wessler, C.J. Kirkpatrick, Acetylcholine beyond neurons: the non-neuronal cholinergic system in humans, Br. J. Pharmacol. 154 (2008), https://doi.org/10.1038/bjp.2008.185.

[10] S.A. Grando, Connections of nicotine to cancer, Nat. Rev. Cancer 14 (2014), https://doi.org/10.1038/nrc3725.

[11] J. Wess, R.M. Eglen, D. Gautam, Muscarinic acetylcholine receptors: mutant mice provide new insights for drug development, Nat. Rev. Drug Discov. 6 (2007), https://doi.org/10.1038/nrd2379.

[12] A. Boss, M. Oppitz, U. Drews, Muscarinic cholinergic receptors in the human melanoma cell line SK-Mel 28: modulation of chemotaxis, Clin. Exp. Dermatol. 30 (2005), https://doi.org/10.1111/j.1365-2230.2005.01865.x.

[13] A.M. Lucianò, A.M. Tata, Functional characterization of cholinergic receptors in melanoma cells, Cancers (Basel) 12 (2020), https://doi.org/10.3390/cancers12113141.

[14] D. Kalamida, K. Poulas, V. Avramopoulou, E. Fostieri, G. Lagoumintzis, K. Lazaridis, A. Sideri, M. Zouridakis, S.J. Tzartos, Muscle and neuronal nicotinic acetylcholine receptors: structure, function and pathogenicity, FEBS J. 274 (2007), https://doi.org/10.1111/j.1742-4658.2007.05935.x.

[15] H.M. Schuller, Is cancer triggered by altered signalling of nicotinic acetylcholine receptors? Nat. Rev. Cancer 9 (2009) https://doi.org/10.1038/nrc2590.

[16] L.C. Huang, C.L. Lin, J.Z. Qiu, C.Y. Lin, K.W. Hsu, K.W. Tam, J.Y. Lee, J.M. Yang, C.H. Lee, Nicotinic acetylcholine receptor subtype alpha-9 mediates triple-negative breast cancers based on a spontaneous pulmonary metastasis mouse model, Front. Cell. Neurosci. 11 (2017), https://doi.org/10.3389/fncel.2017.00336.

[17] C. Schaal, S.P. Chellappan, Nicotine-mediated cell proliferation and tumor progression in smoking-related cancers, Mol. Cancer Res. 12 (2014), https://doi.org/10.1158/1541-7786.MCR-13-0541.

[18] H. Sun, X. Ma, α5-nAChR modulates nicotine-induced cell migration and invasion in A549 lung cancer cells, Exp. Toxicol. Pathol. 67 (2015), https://doi.org/10.1016/j.etp.2015.07.001.

[19] J.C. Qi, W.Y. Xue, Y.P. Zhang, C.B. Qu, B.S. Lu, Y.W. Yin, K.L. Liu, D. bin Wang, W. Li, Z.M. Zhao, Cholinergic α5 nicotinic receptor is involved in the proliferation and invasion of human prostate cancer cells, Oncol. Rep. 43 (2020), https://doi.org/10.3892/or.2019.7411.

[20] N.N. Dang, X. Meng, G. Qin, Y. An, Q.Q. Zhang, X. Cheng, S. Huang, α5-nAChR modulates melanoma growth through the Notch1 signaling pathway, J. Cell. Physiol. 235 (2020), https://doi.org/10.1002/jcp.29435.

[21] H.D. Nguyen, Y.C. Liao, Y.S. Ho, L.C. Chen, H.W. Chang, T.C. Cheng, D. Liu, W. R. Lee, S.C. Shen, C.H. Wu, S.H. Tu, The α9 nicotinic acetylcholine receptor mediates nicotine-induced pd-l1 expression and regulates melanoma cell proliferation and migration, Cancers (Basel) 11 (2019), https://doi.org/10.3390/cancers11121991.

[22] M. Hong, S. Tao, L. Zhang, L.T. Diao, X. Huang, S. Huang, S.J. Xie, Z.D. Xiao, H. Zhang, RNA sequencing: new technologies and applications in cancer research, J. Hematol. Oncol. 13 (2020), https://doi.org/10.1186/s13045-020-01005-x.

[23] J. Fan, K. Slowikowski, F. Zhang, Single-cell transcriptomics in cancer: computational challenges and opportunities, Exp. Mol. Med. 52 (2020), https://doi.org/10.1038/s12276-020-0422-0.

[24] Y. Zhang, D. Wang, M. Peng, L. Tang, J. Ouyang, F. Xiong, C. Guo, Y. Tang, Y. Zhou, Q. Liao, X. Wu, H. Wang, J. Yu, Y. Li, X. Li, G. Li, Z. Zeng, Y. Tan, W. Xiong, Single-cell RNA sequencing in cancer research, J. Exp. Clin. Cancer Res. 40 (2021), https://doi.org/10.1186/s13046-021-01874-1.

[25] I. Tirosh, B. Izar, S.M. Prakadan, M.H. Wadsworth, D. Treacy, J.J. Trombetta, A. Rotem, C. Rodman, C. Lian, G. Murphy, M. Fallahi-Sichani, K. Dutton-Regester, J.R. Lin, O. Cohen, P. Shah, D. Lu, A.S. Genshaft, T.K. Hughes, C.G.K. Ziegler, S. W. Kazer, A. Gaillard, K.E. Kolb, A.C. Villani, C.M. Johannessen, A.Y. Andreev, E. M. van Allen, M. Bertagnolli, P.K. Sorger, R.J. Sullivan, K.T. Flaherty, D. T. Frederick, J. Jané-Valbuena, C.H. Yoon, O. Rozenblatt-Rosen, A.K. Shalek, A. Regev, L.A. Garraway, Dissecting the multicellular ecosystem of metastatic melanoma by single-cell RNA-seq, Science (2016) 352, https://doi.org/10.1126/science.aad0501, 1979.

[26] F. Rambow, A. Rogiers, O. Marin-Bejar, S. Aibar, J. Femel, M. Dewaele, P. Karras, D. Brown, Y.H. Chang, M. Debiec-Rychter, C. Adriaens, E. Radaelli, P. Wolter, O. Bechter, R. Dummer, M. Levesque, A. Piris, D.T. Frederick, G. Boland, K. T. Flaherty, J. van den Oord, T. Voet, S. Aerts, A.W. Lund, J.C. Marine, Toward

[27] L. Jerby-Arnon, P. Shah, M.S. Cuoco, C. Rodman, M.J. Su, J.C. Melms, R. Leeson, A. Kanodia, S. Mei, J.R. Lin, S. Wang, B. Rabasha, D. Liu, G. Zhang, C. Margolais, O. Ashenberg, P.A. Ott, E.I. Buchbinder, R. Haq, F.S. Hodi, G.M. Boland, R. J. Sullivan, D.T. Frederick, B. Miao, T. Moll, K.T. Flaherty, M. Herlyn, R. W. Jenkins, R. Thummalapalli, M.S. Kowalczyk, I. Cañadas, B. Schilling, A.N. R. Cartwright, A.M. Luoma, S. Malu, P. Hwu, C. Bernatchez, M.A. Forget, D. A. Barbie, A.K. Shalek, I. Tirosh, P.K. Sorger, K. Wucherpfennig, E.M. van Allen, D. Schadendorf, B.E. Johnson, A. Rotem, O. Rozenblatt-Rosen, L.A. Garraway, C. H. Yoon, B. Izar, A. Regev, A cancer cell program promotes T cell exclusion and resistance to checkpoint blockade, Cell 175 (2018), https://doi.org/10.1016/j.cell.2018.09.006.

[28] A. Colaprico, T.C. Silva, C. Olsen, L. Garofano, C. Cava, D. Garolini, T.S. Sabedot, T. M. Malta, S.M. Pagnotta, I. Castiglioni, M. Ceccarelli, G. Bontempi, H. Noushmehr, TCGAbiolinks: an R/Bioconductor package for integrative analysis of TCGA data, Nucleic Acids Res. 44 (2016), https://doi.org/10.1093/nar/gkv1507.

[29] D. Sean, P.S. Meltzer, GEOquery: a bridge between the gene expression Omnibus (GEO) and BioConductor, Bioinformatics 23 (2007), https://doi.org/10.1093/bioinformatics/btm254.

[30] M.D. Robinson, D.J. McCarthy, G.K. Smyth, edgeR: a Bioconductor package for differential expression analysis of digital gene expression data, Bioinformatics 26 (2009), https://doi.org/10.1093/bioinformatics/btp616.

[31] S. Durinck, P.T. Spellman, E. Birney, W. Huber, Mapping identifiers for the integration of genomic datasets with the R/Bioconductor package biomaRt, Nat. Protoc. 4 (2009), https://doi.org/10.1038/nprot.2009.97.

[32] M.v. Kuleshov, M.R. Jones, A.D. Rouillard, N.F. Fernandez, Q. Duan, Z. Wang, S. Koplev, S.L. Jenkins, K.M. Jagodnik, A. Lachmann, M.G. McDermott, C. D. Monteiro, G.W. Gundersen, A. Maayan, Enrichr: a comprehensive gene set enrichment analysis web server 2016 update, Nucleic Acids Res. 44 (2016), https://doi.org/10.1093/nar/gkw377.

[33] G. Korotkevich, V. Sukhov, N. Budin, B. Shpak, M.N. Artyomov, A. Sergushichev, Fast gene set enrichment analysis, (n.d.). https://doi.org/10.1101/060012.

[34] P. Shannon, A. Markiel, O. Ozier, N.S. Baliga, J.T. Wang, D. Ramage, N. Amin, B. Schwikowski, T. Ideker, Cytoscape: a software Environment for integrated models of biomolecular interaction networks, Genome Res. 13 (2003), https://doi.org/10.1101/gr.1239303.

[35] N.T. Doncheva, J.H. Morris, J. Gorodkin, L.J. Jensen, Cytoscape StringApp: network analysis and visualization of proteomics data, J. Proteome Res. 18 (2019), https://doi.org/10.1021/acs.jproteome.8b00702.

[36] G.D. Bader, C.W.V. Hogue, An automated method for finding molecular complexes in large protein interaction networks, BMC Bioinf. 4 (2003), https://doi.org/10.1186/1471-2105-4-2.

[37] Z. Tang, C. Li, B. Kang, G. Gao, C. Li, Z. Zhang, GEPIA: a web server for cancer and normal gene expression profiling and interactive analyses, Nucleic Acids Res. 45 (2017), https://doi.org/10.1093/nar/gkx247.

[38] Y. Hao, S. Hao, E. Andersen-Nissen, W.M. Mauck, S. Zheng, A. Butler, M.J. Lee, A. J. Wilk, C. Darby, M. Zager, P. Hoffman, M. Stoeckius, E. Papalexi, E.P. Mimitou, J. Jain, A. Srivastava, T. Stuart, L.M. Fleming, B. Yeung, A.J. Rogers, J. M. McElrath, C.A. Blish, R. Gottardo, P. Smibert, R. Satija, Integrated analysis of multimodal single-cell data, Cell 184 (2021), https://doi.org/10.1016/j.cell.2021.04.048.

[39] S. Hänzelmann, R. Castelo, J. Guinney, GSVA: gene set variation analysis for microarray and RNA-Seq data, BMC Bioinf. 14 (2013), https://doi.org/10.1186/1471-2105-14-7.

[40] Z. Gu, R. Eils, M. Schlesner, Complex heatmaps reveal patterns and correlations in multidimensional genomic data, Bioinformatics 32 (2016), https://doi.org/10.1093/bioinformatics/btw313.

[41] P.M.H. Chang, Y.C. Yeh, T.C. Chen, Y.C. Wu, P.J. Lu, H.C. Cheng, H.J. Lu, M. H. Chen, T.Y. Chou, C.Y.F. Huang, High expression of CHRNA1 is associated with reduced survival in early stage lung adenocarcinoma after complete resection, Ann. Surg Oncol. 20 (2013), https://doi.org/10.1245/s10434-013-3034-2.

[42] D.L. Carlisle, X. Liu, T.M. Hopkins, M.C. Swick, R. Dhir, J.M. Siegfried, Nicotine activates cell-signaling pathways through muscle-type and neuronal nicotinic acetylcholine receptors in non-small cell lung cancer cells, Pulm. Pharmacol. Ther. 20 (2007), https://doi.org/10.1016/j.pupt.2006.07.001.

[43] C. Scherl, R. Schäfer, A. Schlabrakowski, K. Tziridis, H. Iro, O. Wendler, Nicotinic acetylcholine receptors in head and neck cancer and their correlation to tumor site and progression, ORL (Oto-Rhino-Laryngol.) (Basel) 78 (2016), https://doi.org/10.1159/000445781.

[44] R. Spina, D.M. Voss, L. Asnaghi, A. Sloan, E.E. Bar, Atracurium Besylate and other neuromuscular blocking agents promote astroglial differentiation and deplete glioblastoma stem cells, Oncotarget 7 (2016), https://doi.org/10.18632/ONCOTARGET.6314.

[45] G. Richard, S. Dalle, M. Monet, M. Ligier, A. Boespflug, R.M. Pommier, A. Fouchardière, M. Perier-Muzet, L. Depaepe, R. Barnault, G. Tondeur, S. Ansieau, E. Thomas, C. Bertolotto, R. Ballotti, S. Mourah, M. Battistella, C. Lebbé, L. Thomas, A. Puisieux, J. Caramel, ZEB 1-mediated melanoma cell plasticity enhances resistance to MAPK inhibitors, EMBO Mol. Med. 8 (2016), https://doi.org/10.15252/emmm.201505971.

[46] J. Caramel, E. Papadogeorgakis, L. Hill, G.J. Browne, G. Richard, A. Wierinckx, G. Saldanha, J. sborne, P. Hutchinson, G. Tse, J. Lachuer, A. Puisieux, J.H. Pringle, S. Ansieau, E. Tulchinsky, A switch in the expression of embryonic EMT-inducers drives the development of malignant melanoma, Cancer Cell 24 (2013), https://doi.org/10.1016/j.ccr.2013.08.018.

[47] N. Vandamme, G. Denecker, K. Bruneel, G. Blancke, O. Akay, J. Taminau, J. de Coninck, E. de Smedt, N. Skrypek, W. van Loocke, J. Wouters, D. Nittner, C. Kohler, D.S. Darling, P.F. Cheng, M.I.G. Raaijmakers, M.P. Levesque, U.G. Mallya, M. Rafferty, B. Balint, W.M. Gallagher, L. Brochez, D. Huylebroeck, J.J. Haigh, V. Andries, F. Rambow, P. van Vlierberghe, S. Goossens, J.J. van den Oord, J. C. Marine, G. Berx, The EMT transcription factor ZEB2 promotes proliferation of primary and metastatic melanoma while suppressing an invasive, mesenchymal-like phenotype, Cancer Res. 80 (2020), https://doi.org/10.1158/0008-5472.CAN-19-2373.

[48] G. Denecker, N. Vandamme, Ö. Akay, D. Koludrovic, J. Taminau, K. Lemeire, A. Gheldof, B. de Craene, M. van Gele, L. Brochez, G.M. Udupi, M. Rafferty, B. Balint, W.M. Gallagher, G. Ghanem, D. Huylebroeck, J. Haigh, J. van den Oord, L. Larue, I. Davidson, J.C. Marine, G. Berx, Identification of a ZEB2-MITF-ZEB1 transcriptional network that controls melanogenesis and melanoma progression, Cell Death Differ. 21 (2014), https://doi.org/10.1038/cdd.2014.44.

[49] J.R. King, N. Kabbani, Alpha 7 nicotinic receptor coupling to heterotrimeric G proteins modulates RhoA activation, cytoskeletal motility, and structural growth, J. Neurochem. (2016), https://doi.org/10.1111/jnc.13660.

[50] X. Yang, H. Ren, X. Guo, C. Hu, J. Fu, The expressions and mechanisms of sarcomeric proteins in cancers, Dis. Markers 2020 (2020), https://doi.org/10.1155/2020/8885286.

[51] Y. Ma, J. Peng, W. Liu, P. Zhang, L. Huang, B. Gao, T. Shen, Y. Zhou, H. Chen, Z. Chu, M. Zhang, H. Qin, Proteomics identification of desmin as a potential oncofetal diagnostic and prognostic biomarker in colorectal cancer, Mol. Cell. Proteomics 8 (2009), https://doi.org/10.1074/mcp.M800541-MCP200.

[52] S. Bhunia, M.A. Barbhuiya, S. Gupta, B.R. Shrivastava, P.K. Tiwari, Epigenetic downregulation of desmin in gall bladder cancer reveals its potential role in disease progression, Indian J. Med. Res. 151 (Supplement) (2020), https://doi.org/10.4103/ijmr.IJMR_501_18.

[53] G. Arentz, T. Chataway, T.J. Price, Z. Izwan, G. Hardi, A.G. Cummins, J. E. Hardingham, Desmin expression in colorectal cancer stroma correlates with advanced stage disease and marks angiogenic microvessels, Clin. Proteomics 8 (2011), https://doi.org/10.1186/1559-0275-8-16.

[54] S. Stauffer, Y. Zeng, J. Zhou, X. Chen, Y. Chen, J. Dong, CDK1-mediated mitotic phosphorylation of PBK is involved in cytokinesis and inhibits its oncogenic activity, Cell. Signal. 39 (2017), https://doi.org/10.1016/j.cellsig.2017.08.001.

[55] M.F. Gayyed, N.M.R.A. El-Maqsoud, E.R. Tawfiek, S.A.A. el Gelany, M.F. A. Rahman, A comprehensive analysis of CDC20 overexpression in common malignant tumors from multiple organs: its correlation with tumor grade and stage, Tumor Biol. 37 (2016), https://doi.org/10.1007/s13277-015-3808-1.

[56] J. Li, Y. Wang, X. Wang, Q. Yang, CDK1 and CDC20 overexpression in patients with colorectal cancer are associated with poor prognosis: evidence from integrated bioinformatics analysis, World J. Surg. Oncol. 18 (2020), https://doi.org/10.1186/s12957-020-01817-8.

[57] M. Kamil, Y. Shinsato, N. Higa, T. Hirano, M. Idogawa, T. Takajo, K. Minami, M. Shimokawa, M. Yamamoto, K. Kawahara, H. Yonezawa, H. Hirano, T. Furukawa, K. Yoshimoto, K. Arita, High filamin-C expression predicts enhanced invasiveness and poor outcome in glioblastoma multiforme, Br. J. Cancer 120 (2019), https://doi.org/10.1038/s41416-019-0413-x.

[58] B. Yang, Y. Liu, J. Zhao, K. Hei, H. Zhuang, Q. Li, W. Wei, R. Chen, N. Zhang, Y. Li, Ectopic overexpression of filamin C scaffolds MEK1/2 and ERK1/2 to promote the progression of human hepatocellular carcinoma, Cancer Lett. 388 (2017), https://doi.org/10.1016/j.canlet.2016.11.037.

[59] K. Tanabe, Y. Shinsato, T. Furukawa, Y. Kita, K. Hatanaka, K. Minami, K. Kawahara, M. Yamamoto, K. Baba, S. Mori, Y. Uchikado, K. Maemura, A. Tanimoto, S. Natsugoe, Filamin C promotes lymphatic invasion and lymphatic metastasis and increases cell motility by regulating Rho GTPase in esophageal squamous cell carcinoma, Oncotarget 8 (2017), https://doi.org/10.18632/oncotarget.14087.